Journal of Food and Nutrition Research, 2021, Vol. 9, No. 8, 434-441
Available online at http://pubs.sciepub.com/jfnr/9/8/6
Published by Science and Education Publishing
DOI:10.12691/jfnr-9-8-6

Bangle (*Zingiber purpureum*) Extract Attenuates Insulin Resistance and Inflammation in the Skeletal Muscle of High Fat Diet-fed Young SAMP8 Mice

Shin Sato[1,*], Nagomi Takahashi[1], Yuuka Mukai[2]

[1]Department of Nutrition, Faculty of Health Science, Aomori University of Health and Welfare, Aomori 030-8505, Japan
[2]School of Nutrition and Dietetics, Faculty of Health and Social Work,
Kanagawa University of Human Services, Kanagawa 238-8522, Japan
*Corresponding author: s_sato3@auhw.ac.jp

Received July 12, 2021; Revised August 17, 2021; Accepted August 25, 2021

Abstract Insulin resistance induced by chronic inflammation enhances metabolic dysfunction in obesity. The aim of this study was to investigate the effects of Bangle (*Zingiber purpureum*) extract (Ba) on insulin resistance and inflammation in the gastrocnemius muscle (GM) of high-fat diet (HFD)-fed SAMP8 mice. Male mice were divided into three groups: HFD, HFD + 1%Ba, and + 2%Ba. The SAMP8 control (Con) and SAMR1 control (Rcon) were fed a low-fat diet. At week 26, plasma blood parameters, macrophage infiltration, levels of expression and phosphorylation of Akt, mTOR, and AMPK were examined. The levels of plasma glucose and insulin in the HFD group were significantly higher than those in the Con group. Conversely, these levels in the HFD + 2%Ba group were significantly lower than those in the HFD group. Treatment with 2% Ba suppressed the degree of macrophage infiltration induced by HFD in the GMs. The levels of phosphorylated Akt and mTOR were decreased and the levels of phosphorylated AMPK in the HFD + 2%Ba group were increased compared with those in the HFD group. Ba may attenuate HFD-induced insulin resistance and inflammation by modulating the AMPK/Akt/mTOR pathway in the GMs of HFD-fed young SAMP8 mice.

Keywords: *bangle, insulin resistance, inflammation, skeletal muscle, high fat diet*

Cite This Article: Shin Sato, Nagomi Takahashi, and Yuuka Mukai, "Bangle (*Zingiber purpureum*) Extract Attenuates Insulin Resistance and Inflammation in the Skeletal Muscle of High Fat Diet-fed Young SAMP8 Mice." *Journal of Food and Nutrition Research*, vol. 9, no. 8 (2021): 434-441. doi: 10.12691/jfnr-9-8-6.

1. Introduction

A high-fat diet (HFD) intake increases the circulation of non-esterified fatty acids, resulting in insulin resistance in the liver, adipose tissues, and skeletal muscle [1]. Chronic inflammation in metabolic tissues is involved in the onset and/or progression of insulin resistance [2]. In addition, insulin resistance induced by chronic inflammation may enhance metabolic dysfunction in the skeletal muscle in type 2 diabetes mellitus [3]. In animal models, chronic inflammation and macrophage markers in the skeletal muscle are increased and associated with insulin resistance [4]. Moreover, chronic inflammation is associated with apoptosis induction [5]. In addition, aging is associated with chronic inflammation concomitant with increased plasma levels of pro-inflammatory mediators such as tumor necrosis factor (TNF)-α and interleukin (IL)-6 in sarcopenic elderly people [6], suggesting that these mediators affect insulin resistance as well as protein metabolism in skeletal muscle with aging. Therefore, chronic inflammation and/or insulin resistance in the skeletal muscle may be potential therapeutic targets for the prevention of age-related wasting of muscles.

Obesity-related insulin resistance is associated with the regulation of insulin signaling pathway by proteins including phosphoinositide 3-kinase (PI3K) and Akt [7]. In skeletal muscles, mammalian target of rapamycin (mTOR), which senses various environmental and intracellular changes, including nutrient availability and energy status [8], regulates muscle mass, resulting in the modulation of muscle hypertrophy and muscle wastage [9]. The increase in Akt and mTOR activity is associated with the development of insulin resistance in skeletal muscles [10,11]. For instance, Lepidium sativum seed extract attenuates insulin resistance and hepatic inflammation in HFD-fed rats through the regulation of Akt/mTOR signaling [12]. AMP-activated protein kinase (AMPK) is known to regulate various physiological events, including cellular growth and proliferation, mitochondrial function, and factors linked to insulin resistance, inflammation, and oxidative stress [13]. For instance, AMPK activation improves inflammation and insulin resistance in the skeletal muscle and adipose tissue of women with gestational diabetes mellitus and normal glucose tolerance [14]. When HFD-fed mice received dietary red raspberry,

the inflammatory responses and sensitizing insulin signaling were alleviated in the skeletal muscle through the activation of AMPK [15]. Thus, stimulation of the AMPK/Akt/mTOR pathway is expected to alter inflammation and insulin resistance in the skeletal muscle of obese or elderly people.

Bangle (*Zingiber purpureum*) is a tropical ginger widely distributed in Southeast Asia. In Indonesia, Bangle is known to be a spice and a traditional medicine to treat fever and headaches. Bangle extract improves spatial learning and reduces deficits in memory in senescence-accelerated mice [16]. However, the protective effects of Bangle on chronic inflammation and insulin resistance in skeletal muscles are not fully understood. Therefore, the aim of the present study was to examine whether Bangle extract (Ba) could improve insulin resistance and inflammation, and whether Ba stimulates the AMPK/Akt/mTOR pathway in the gastrocnemius muscle (GM) of HFD-fed senescence-accelerated prone mice (SAMP8).

2. Materials and Methods

2.1. Bangle Extract

The Bangle extract (Ba) powder contained trans- and cis-3-(3',4'-dimethoxyphenyl)-4-[(E)-3",4"-dimethoxystyryl]cyclohex-1-ene (phenylbutenoid dimers; 5.0%) (Figure 1) and composed of Ba 20.2%, emulsifier 8.5%, and dextrin 71.3%. The Ba powder was kindly supplied by Hosoda SHC Co. (Fukui, Japan).

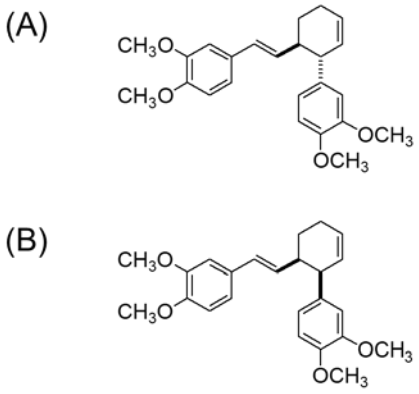

Figure 1. Structural features of phenylbutenoid dimers, trans-3-(3',4'-dimethoxyphenyl)-4-[(E)-3",4"-dimethoxystyryl]cyclohex-1-ene (A) and cis-3-(3',4'-dimethoxyphenyl)-4-[(E)-3",4"-dimethoxystyryl]cyclohex-1-ene (B)

2.2. Animal Treatments

All procedures were performed in accordance with the regulations of the Guidelines for Animal Experimentation, Aomori University of Health and Welfare (Permission number: 17004). The animal experiments described in the article have been carried out in accordance with EU directive for animal experiments and the relevant national guides on the care and use of laboratory animals ("Act on Welfare and Management of Animals" in Japan). Four-week-old male SAMP8 and R1 (Japan SLC, Inc., Shizuoka, Japan), weighing 21.6–23.3 g and 19.7–25.0 g, were used, respectively. After 4 weeks of adaptation maintenance, SAMP8 received diets providing 45% of energy from fat (HFD; n = 22) and 13% of energy from fat (LFD; n = 8, SAMP8 control (Con) group) for 8 weeks. To confirm the effect of HFD intake on body weight gain, all mice received LFD for 2 weeks. SAMR1 control (Rcon; n = 6) was fed a diet that provided 13% of energy from fat. Thereafter, the mice that received a HFD were randomly divided into three groups, where n indicates the number of animals in each group: 0% Bangle extract (Ba) (HFD + 0% Ba; n = 8), 1% Ba (HFD + 1% Ba; n = 6), and 2% Ba (HFD + 2% Ba; n = 8). The rest of SAMP8 (Con; n = 8) was fed a diet providing 13% of energy from fat during the treatments. All mice were maintained at a constant temperature of 23 ± 1 °C under a 12 h light/dark cycle and were fed the corresponding diets and distilled water ad libitum. Before the mice were euthanized at week 26, all animals were fasted overnight (15–16 h), weighed, and blood samples were collected from the abdominal aorta under anesthesia. The GMs and epididymal fat tissue were quickly removed, and fixed in 4% paraformaldehyde phosphate buffer solution for immunohistochemistry. Portions of the GMs were immediately frozen in liquid nitrogen and stored at -80°C until use.

2.3. Plasma Biochemical Parameters

Plasma samples were separated by centrifugation, and tested for glucose (Glc), triacylglycerol (Tg), and non-esterified fatty acid (NEFA) levels using a commercially available kit. Plasma insulin levels were measured using the LBIS Mouse Insulin ELISA Kit (AKRIN-011RU, FUJIFILM Wako Shibayagi Corporation, Gunma, Japan). Homeostatic model assessment insulin resistance (HOMA-IR), a biomarker of insulin sensitivity, was determined using the following equation [17]:

$$HOMA-IR=\begin{bmatrix}26\times fasting\ insulin\left(ng/ml\right)\\ \times fasting\ glu\cos e\left(ng/ml\right)\end{bmatrix}/405$$

2.4. Histopathology and Immunohistochemistry

Paraformaldehyde-fixed GMs and epididymal fat tissues were embedded in paraffin, and were stained with collagen fibrils using a Sirius red/Fast green collagen staining kit (Chondrex, Inc., Redmond, WA, USA). After 10 randomly selected fields per animal were chosen, the Sirius red-stained area was measured, and normalized to the total cross-sectional area and expressed as a percentage. The GM sections were stained for macrophages as described in a previous study [18]. Briefly, deparaffinized sections were pre-treated with pepsin solution and hydrogen peroxide (H_2O_2) and subsequently pre-incubated with skimmed milk in PBS and incubated with F4/80 antibody (1:60, Bio-Rad Laboratories, Inc., Hercules, CA, USA). The sections were incubated with Histofine Simple Stain Mouse MAX PO (Nichirei Biosciences Inc., Tokyo, Japan), and positive reactions were visualized using 3,3'-diaminobenzidine tetrahydrochloride in 50 mM Tris-HCl buffer containing H2O2. For the measurement of F4/80-immunopositive cells in the GM and epididymal fat tissue, 10 randomly selected fields were chosen.

Quantification was performed using CellSensDimension software (Olympus Corporation, Tokyo, Japan).

2.5. Western Blot Analysis

The GMs were homogenized in homogenizing buffer (50 mM N-2-hydroxyethylpiperazine-N'-2-ethanesulphonic acid [HEPES], 150 mM NaCl, 1 mM dithiothreitol, and 0.5% (v/v) Tween 20, pH 7.4) supplemented with a protease inhibitor cocktail (Roche Applied Science, Indianapolis, IN, USA). The homogenates were centrifuged. The protein concentrations in the supernatants were determined. Standard western blotting techniques were performed for protein analyses as described in a previous report [18]. The proteins were electrophoresed on SDS-PAGE and subsequently electrotransferred onto polyvinylidene difluoride (PVDF) membranes. The membranes were blocked and incubated with a rabbit AMPK antibody, phospho-AMPK-Thr^{172}, Akt, phospho-Akt-Ser^{473}, mTOR, phospho-mTOR-Ser^{2448}, and cleaved caspase 3 (Cell Signaling Technology, Danvers, MA, USA). After washing, the membranes were incubated with the appropriate secondary horseradish peroxidase-conjugated antibodies. Protein bands were visualized using ECL western blotting Detection Reagents (GE Healthcare UK Ltd., Buckinghamshire, UK) on Hyperfilm (GE Healthcare UK Ltd.). The specific band density was quantitatively analysed. Protein levels were normalized using the formula that the band density of the target protein was divided by that of glyceraldehyde-3-phosphate dehydrogenase (GAPDH).

2.6. Statistical Analysis

Each value is expressed as the mean ± SEM. Statistical analyses were performed using one-way analysis of variance, followed by Tukey's test. In all cases, statistical significance was set at $P < 0.05$.

3. Results

3.1. Body, feed intake, and tissue weights

The body weights of the HFD-fed groups were significantly higher than those of the Con (LFD-fed SAMP8) group from weeks 21 to 26 (Figure 2). Although no significant difference was found among the body weights of the HFD + 0% Ba, 1% Ba, and 2% Ba groups, the body weights of the 2% Ba group tended to be lower than those of the 0% Ba group at week 26 (P = 0.349). No significant difference was observed in the feed intake of the HFD + 0% Ba, 1% Ba, and 2% Ba groups at weeks 20, 22, and 24 (Table 1). The relative GM weights in the HFD + 0% Ba, 1% Ba, and 2% Ba groups were significantly lower than those of the Rcon (LFD-fed SAMR1) and Con groups, respectively (Table 2). There was no significant difference in the relative GM weights among the HFD + 0% Ba, 1% Ba, and 2% Ba groups. The relative epididymal fat tissue weights in the HFD + 0% Ba, 1% Ba, and 2% Ba groups were significantly higher than those in the Con group. The relative weights of perirenal fat tissue in the HFD + 0% Ba group were significantly higher than those in the Con group. Conversely, the relative weights in the 2% Ba group were significantly lower than those in the 0% Ba group.

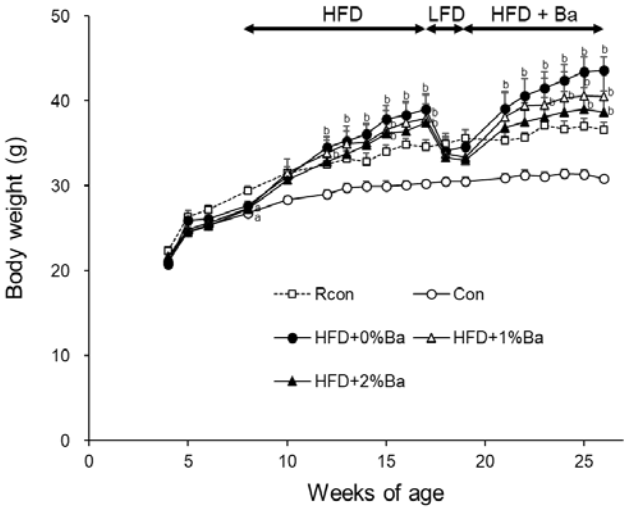

Figure 2. Effects of Bangle extract (Ba) on body weights in SAMP8 mice fed a high-fat diet (HFD). Values are expressed as mean ± SEM (n = 5–8). $^{a}P < 0.05$ compared with Rcon (SAMR1 control) group. $^{b}P < 0.05$ compared with Con (SAMP8 control) group

Table 1. Effect of Bangle extract on food intake (gram per 2 rats per day) in SAMP8 fed a high-fat diet

	Rcon	Con	High-fat diet		
			0%Ba	1%Ba	2%Ba
Week 20	9.3±0.2	9.8±0.3	15.1±1.7^{a,b}	11.6±0.6	15.0±0.8^{a,b}
Week 22	8.5±0.3	10.1±0.5	11.8±1.0	12.3±1.3	12.9±1.6
Week 24	9.3±0.5	10.2±0.3	9.8±3.2	11.7±0.4	12.1±1.4
Week 25	8.6±0.4	8.8±0.6	15.1±1.1^{a,b}	10.5±0.2^{c}	12.4±1.9

Values are means ± SEM (n = 4-5). $^{a}P < 0.05$ compared with Rcon group. $^{b}P < 0.05$ compared with Con group. $^{c}P < 0.05$ compared with HFD+0%Ba group. Rcon, SAMR1; Con, SAMP8 ; Ba, Bangle extract.

Table 2. Effect of Bangle extract treatment on tissue weights in SAMP8 fed a high-fat diet

	Rcon	Con	High-fat diet		
			0%Ba	1%Ba	2%Ba
Body weight (g)†	34.6±0.8	28.6±0.3	41.1±1.7^{b}	38.3±2.9^{b}	36.8±2.4^{b}
Gastrocnemius muscle (g)	0.375±0.008	0.303±0.005^{a}	0.337±0.010	0.320±0.014^{a}	0.312±0.008^{a}
Epididymal fat tissue (g)	1.040±0.156	0.283±0.029^{a}	1.689±0.132^{a,b}	1.574±0.186^{b}	1.235±0.143^{b}
Perirenal fat tissue (g)	0.353±0.053	0.107±0.012^{a}	0.677±0.063^{a,b}	0.566±0.070^{b}	0.444±0.052^{b,c}
Gastrocnemius muscle/BW (g/kg)	10.85±0.35	10.62±0.14	8.28±0.37^{a,b}	8.48±0.40^{a,b}	8.63±0.37^{a,b}
Epididymal fat tissue/BW (g/kg)	26.65±3.89	9.85±0.92^{a}	41.04±2.87^{a,b}	40.45±2.58^{a,b}	32.89±1.95^{b}
Perirenal fat tissue/BW (g/kg)	10.08±1.34	3.71±0.39^{a}	16.24±1.06^{a,b}	14.77±1.45^{a,b}	11.83±0.67^{b,c}

†At sacrifice. Values are means ± SEM (n = 6-8). $^{a}P < 0.05$ compared with Rcon group. $^{b}P < 0.05$ compared with Con group. $^{c}P < 0.05$ compared with HFD group (0% Ba). Rcon, SAMR1; Con, SAMP8 ; Ba, Bangle extract.

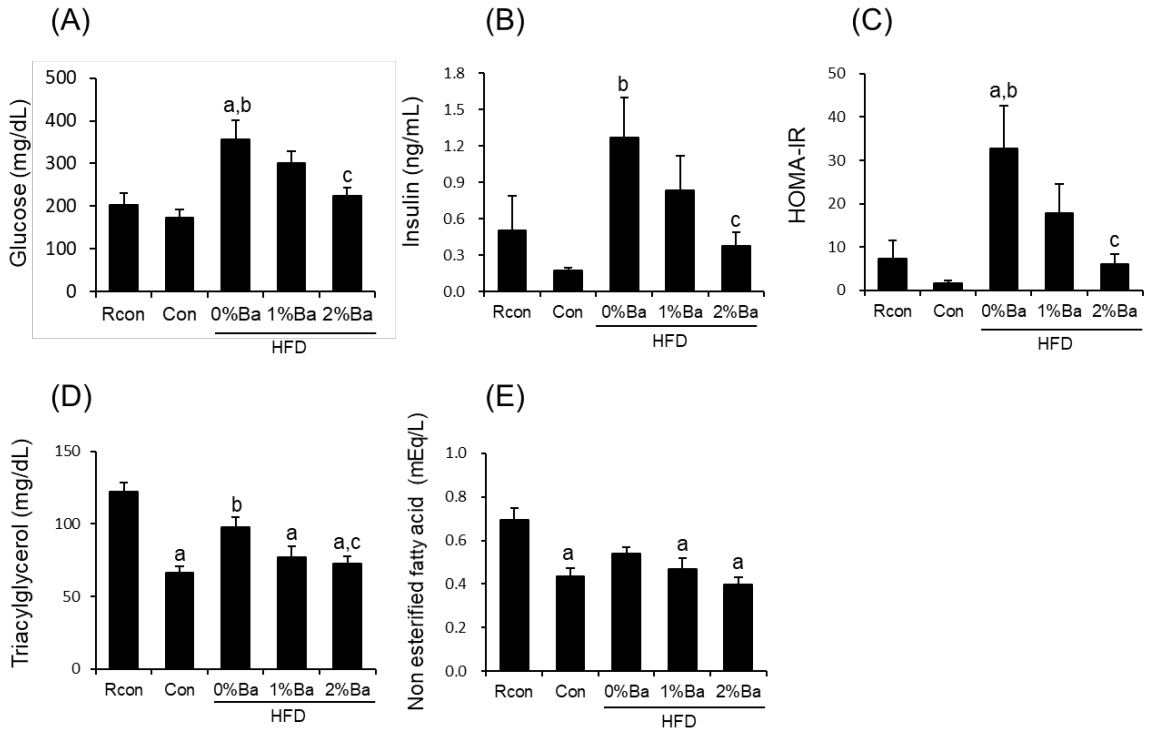

Figure 3. Effects of Bangle extract (Ba) on plasma parameters in SAMP8 mice fed a high-fat diet (HFD). (A) glucose, (B) insulin, (C) homeostatic model assessment of insulin resistance (HOMA-IR), (D) triacylglycerol, and (E) non-esterified fatty acid. Values are expressed as mean ± SEM (n = 5–8). [a]$P < 0.05$ compared with Rcon (SAMR1 control) group. [b]$P < 0.05$ compared with Con (SAMP8 control) group. [c]$P < 0.05$ compared with HFD+0% Ba group. [d]$P < 0.05$ compared with HFD+1% Ba group

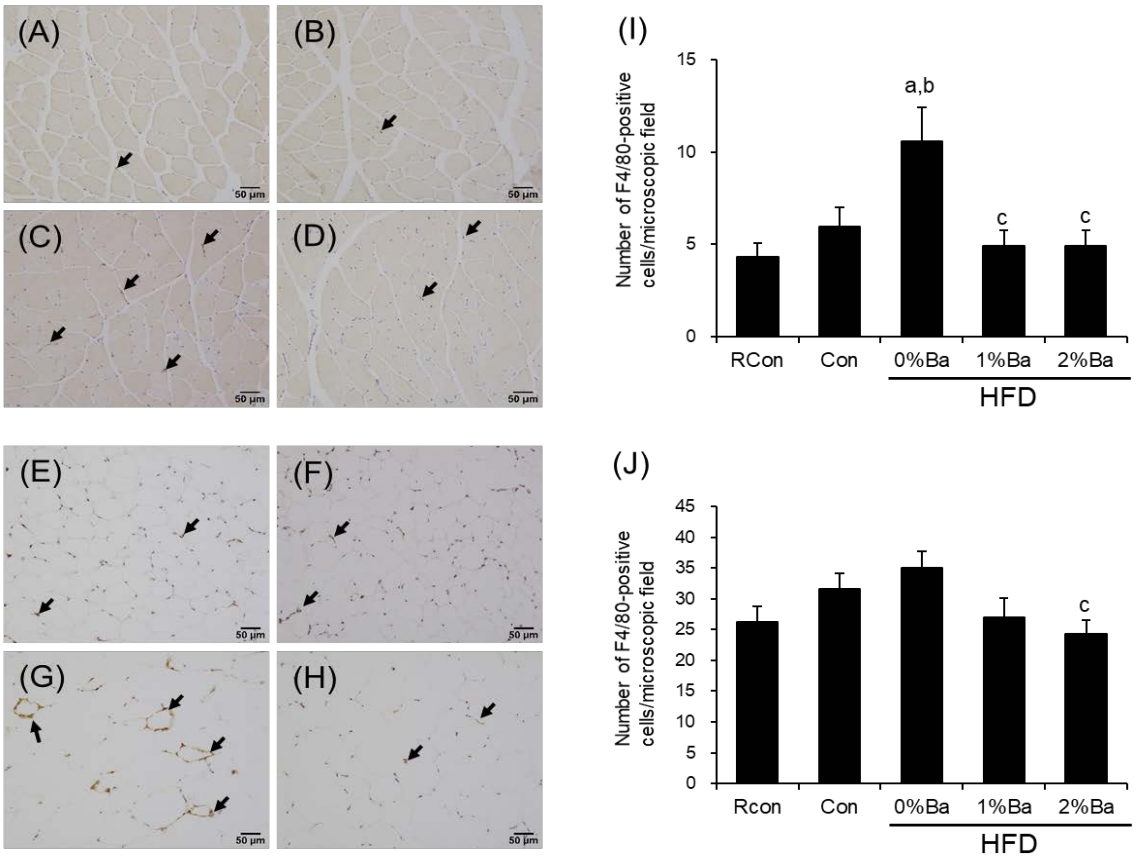

Figure 4. Effects of Bangle extract (Ba) on macrophage infiltration in the gastrocnemius muscle (GM) and epididymal fat tissues of high-fat diet (HFD) fed SAMP8 mice. Representative images of immunohistochemical staining for mouse macrophage-specific F4/80 in the GMs (A, B, C, and D) and epididymal fat tissues (E, F, G, and H), respectively. (A, E); Rcon (SAMR1 control), (B, F); Con (SAMP8 control), (C, G); HFD + 0% Ba, and (D, H); HFD + 2% Ba groups. Number of F4/80-positive macrophages in (I) GMs and (J) epididymal fat tissues. Arrows indicate F4/80-positive macrophages. Counterstaining with hematoxylin (scale bar: 50 μm for all images). Values are presented as the mean ± SEM (n = 6–8). [a]$P < 0.05$ compared with Rcon group. [b]$P < 0.05$ compared with Con group. [c]$P < 0.05$ compared with HFD + 0% Ba

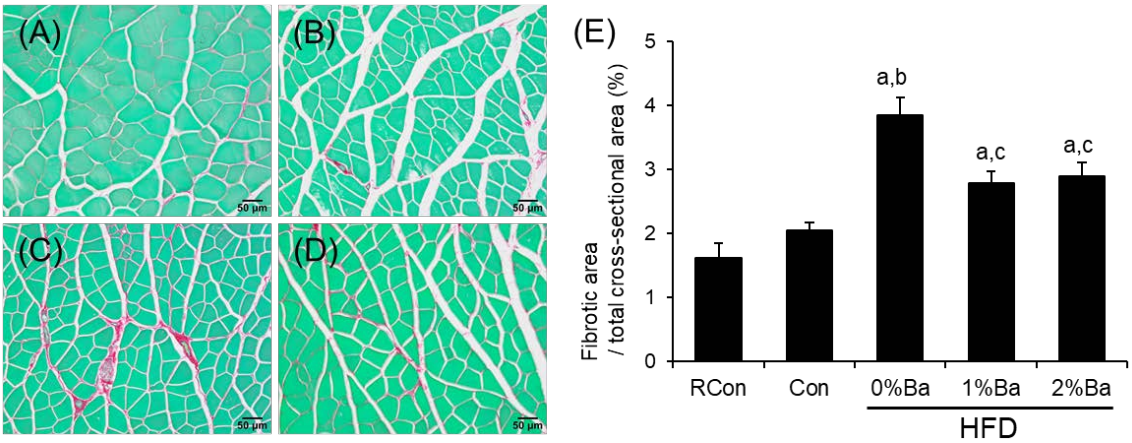

Figure 5. Effects of Bangle extract (Ba) on Sirius-red-stained fibrotic areas in the gastrocnemius muscle (GM) of high-fat diet (HFD)-fed SAMP8 mice. (A) Rcon (SAMR1 control), (B) Con (SAMP8 control), (C) HFD + 0% Ba, and (D) HFD + 2% Ba groups. Sirius-red-staining was carried out (Original magnification 200×, Scale bar: 50 μm). Percentage area of fibrosis per total cross-sectional area (E). Values are presented as mean ± SEM (n = 5–8). ^{a}P < 0.05 compared with Rcon group. ^{b}P < 0.05 compared with Con group. ^{c}P < 0.05 compared with HFD+0%Ba group

3.2. Plasma Biochemical Parameters and Insulin Levels

The levels of plasma Glc and insulin in the HFD + 0% Ba group were significantly higher than those in the Con group. In contrast, the levels in the HFD + 2% Ba group were significantly lower than those in the 0% Ba group (Figure 3). Likewise, the HOMA-IR levels in the HFD + 0% Ba group increased significantly compared to those in the Con group. Conversely, the HOMA-IR levels in the HFD + 2% Ba group were significantly lower than those in the 0% Ba group, indicating that the 2% Ba treatment may attenuate insulin resistance in HFD-fed mice. The plasma Tg levels in the HFD + 0% Ba group were significantly higher than those in the Con group. Conversely, the levels in the HFD + 2% Ba group were significantly lower than those in the 0% Ba group (Figure 3).

3.3. Effect of Ba on Macrophages Infiltration and Sirius-red-stained Fibrotic Areas

Fewer F4/80-positive macrophages were observed in the GM and epididymal fat tissue of the HFD + 2% Ba group, compared with the HFD + 0% Ba group. To examine the effect of Ba treatment on macrophage infiltration in the GM and epididymal fat tissue, F4/80-positive macrophages were counted. The number of macrophages in the GM of the HFD + 0% Ba group was significantly higher than that in the Con group (Figure 4). Conversely, the macrophage numbers in the HFD + 1% Ba and 2% Ba groups were significantly lower than those in the HFD + 0% Ba group. The number of macrophages in the epididymal fat tissue did not differ significantly among the Rcon, Con, and HFD + 0% Ba groups (Figure 4). However, the macrophage numbers in the HFD+2% Ba group were significantly lower than those in the 0% Ba group. These results indicate that Ba treatment attenuated macrophage infiltration into the skeletal muscles and adipose tissues of HFD-fed mice treated with 2% Ba.

Representative Sirius red-stained GM sections from HFD-fed mice treated with Ba are shown in Figure 5. The percentage area of fibrosis per total cross-sectional area in the HFD + 0% Ba group was significantly higher than that in the Con group (Figure 5). Conversely, the fibrotic areas in the GMs of HFD + 1% Ba and 2% Ba groups decreased significantly compared to the levels in the HFD + 0% Ba group, indicating that Ba suppresses the increased fibrotic areas in the GMs of HFD-fed mice.

3.4. Effect of Ba on the Levels of Cleaved Caspase 3

Because chronic inflammation is related to the induction of apoptosis, we determined the cleavage levels of caspase 3, which is involved in the apoptotic pathway. The levels of cleaved caspase 3 in the GMs of the Con group tended to be higher than those in the Rcon group (P = 0.246) (Figure 6). This result suggests that apoptosis might be induced in the skeletal muscles, even in young SAMP8 mice. The levels of cleaved caspase 3 in the HFD + 0% Ba group were similar to those in the Con group (Figure 6). Conversely, the expression in the HFD + 2% Ba group was significantly lower than that in the HFD + 0% Ba group, indicating that Ba treatment suppressed obesity-related apoptosis in the GMs of HFD-fed mice.

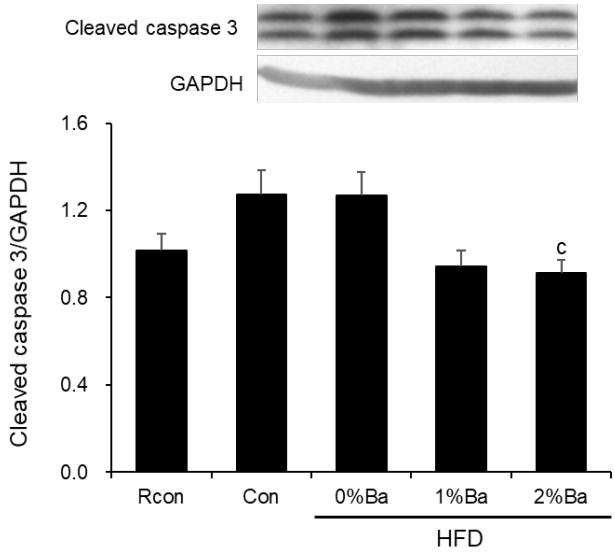

Figure 6. Effects of Bangle extract (Ba) on cleaved caspase 3 levels in the gastrocnemius muscle (GM) of high-fat diet (HFD)-fed SAMP8 mice. Values are presented as the mean ± SEM (n = 6–8). ^{c}P < 0.05 compared with HFD + 0% Ba

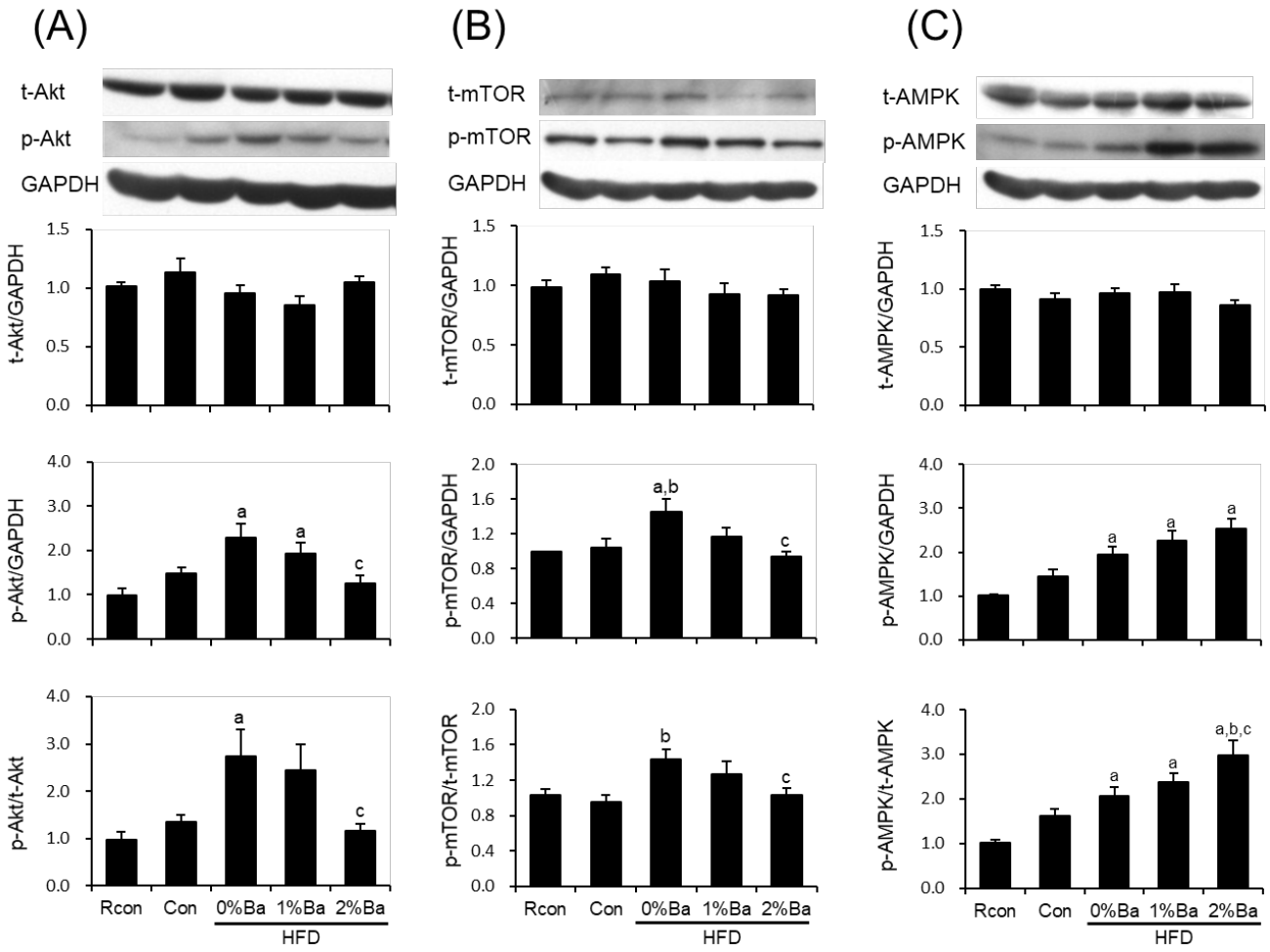

Figure 7. Effect of Bangle extract (Ba) on the expression and phosphorylation of Akt (A), mammalian target of rapamycin (mTOR) (B), and AMP-activated protein kinase (AMPK) (C) in the gastrocnemius muscle (GM) of SAMP8 mice fed a high-fat diet (HFD). Values are presented as the mean ± SEM (n = 6–8). [a]$P < 0.05$ compared with Rcon (SAMR1 control) group. [b]$P < 0.05$ compared with Con (SAMP8 control) group. [c]$P < 0.05$ compared with HFD + 0% Ba

3.5. Effect of Ba Treatment on the Expression and Phosphorylation of Akt, mTOR, and AMPK

The levels of phosphorylated Akt in the HFD + 0% Ba group tended to be higher than that in the Con group (P = 0.061) (Figure 7A). Conversely, the levels in the HFD + 2% Ba group were significantly lower than those in the HFD + 0% Ba group. Likewise, the levels of p-Akt/t-Akt ratio in the HFD + 2% Ba group were significantly lower than those in the HFD + 0% Ba group. The levels of phosphorylated mTOR and p-mTOR/t-mTOR ratio in the HFD + 0% Ba group were higher than those in the Con group. Conversely, these levels in the HFD + 2% Ba group were significantly lower than those in the HFD + 0% Ba group (Figure 7B). The levels of phosphorylated AMPK in the HFD + 0% Ba, 1% Ba, and 2% Ba groups were significantly higher than those in the Con group. The levels of p-AMPK/t-AMPK ratio in the HFD + 2% Ba group were significantly higher than those in the HFD + 0% Ba group (Figure 7C), indicating that Ba treatment upregulated AMPK activation in the GMs of HFD-fed mice.

4. Discussion

The major findings of the present study in the HFD+Ba-fed young SAMP8 mice were as follows: (i) the plasma levels of glucose and insulin were decreased, (ii) the macrophage number and the fibrotic areas were decreased, (iii) the levels of cleaved caspase 3 were decreased, and (iv) Akt and mTOR phosphorylation were downregulated while AMPK phosphorylation was upregulated in the GMs compared with the HFD-fed SAMP8 mice.

In this study, we found that, in glucose metabolism, significantly higher plasma levels of Glc and insulin were found in the HFD-fed mice than in the control SAMP8 mice. These results are consistent with a previous report that HFD-fed mice showed increased insulin secretion and impaired glucose tolerance [19]. Conversely, these levels in the HFD + Ba-fed mice were consistently lower than those in the HFD-fed mice. In addition, we noted that the index of HOMA-IR, which is known to be a valid measure to determine insulin resistance induced by an HFD [17], was reduced in the HFD + Ba-fed mice compared with that in the HFD mice. Furthermore, the relative perirenal

fat tissue weights in the HFD-fed mice treated with Ba were significantly decreased, and that the relative epididymal fat tissue weights tended to be lower than those in the HFD-fed mice. The plasma levels of Tg in the HFD-fed mice treated with Ba were significantly lower than those in the HFD-fed mice. Therefore, the treatment with Ba was suggested to be effective in preventing insulin resistance as well as the dysfunction of lipid metabolism induced by HFD. In addition, we confirmed that the levels of plasma Tg and NEFA in the Con group were lower than those in the Rcon group. Decreased lipid absorption was reported to be due to reduced pancreatic lipase activity in aging mice [20], suggesting that the decreased plasma levels of Tg and NEFA may be affected by age-related lipid metabolism in SAMP8 even at week 26.

This study demonstrated that Ba treatment decreased the macrophage number and the percentage of fibrotic area, concomitant with a downregulation of cleaved caspase 3 levels in the GMs of HFD-fed mice. In skeletal muscles, obesity is associated with the induction of myocyte inflammation, which adversely regulates myocyte metabolism, leading to insulin resistance [3]. Zingerone, a key phenolic compound found in ginger (*Zingiber officinale*), has been reported to decrease collagen deposition and inflammatory activities such as TNF-α and IL-1β levels in bleomycin-induced pulmonary fibrosis in rats [21], and to reduce myocardial fibrosis and inflammation in streptozotocin-induced diabetic rats [22]. Zerumbone, a major component of ginger (*Zingiber zerumbet*), also inhibits the production of pro-inflammatory cytokines in lipopolysaccharide (LPS)-activated inflammation of human monocyte-derived macrophages [23]. In addition, chronic inflammation is closely associated with the initiation of fibrosis and apoptosis, leading to the impairment of insulin resistance [24]. Thus, the treatment of Ba may contribute to the attenuation of macrophage infiltration and decreased fibrosis, concomitant with the inhibition of apoptosis in the skeletal muscle of HFD-fed mice.

Interestingly, this study demonstrated that Ba upregulated AMPK activation in the GM of HFD-fed mice. The ethanol extract from the rhizome of ginger (*Zingiber zerumbet*) upregulated AMPK phosphorylation in the kidneys of diabetic rats [25]. In addition, ginger extract upregulated Glut 4 expression via the AMPK pathway in C2C12 myoblast cells [26]. Ginger (*Zingiber officinale*) extract promotes mitochondrial biogenesis through the activation of AMPK in the muscle and liver of mice [27]. Furthermore, AMPK activation was associated with inflammation. For instance, metformin, which is known as an antidiabetic drug, is reported to ameliorate low-grade inflammation through the activation of AMPK in HFD-fed mice [28]. Therefore, Ba treatments may be involved in the improvement of glucose metabolism as well as chronic inflammation in the GMs through the activation of AMPK.

This study showed an increase in phosphorylated Akt and mTOR levels in the GMs of HFD-fed mice. Although the Akt/mTOR pathway is considered to be essential for muscle hypertrophy [29], the sustained activation of mTOR complex 1 (mTORC1) is reported to lead to abnormal mitochondria, oxidative stress, and damage and loss of fibers [30]. In addition, the increased activation of mTOR in the skeletal muscle and liver is involved in obesity-related insulin resistance [10]. Moreover, diet-induced obesity increases vascular dysfunction through long-term activation of the Akt/mTOR pathway [31]. Notably, we demonstrated that the increased phosphorylation of Akt and mTOR decreased in the GMs of HFD-fed mice treated with Ba. Zingerone attenuated cell proliferation by inhibiting the PI3K/Akt/mTOR pathway in human prostate cancer PC3 cells [32]. In addition, resveratrol, a natural polyphenol, suppresses fatty acid-induced insulin resistance by increasing AMPK activity and inhibiting mTOR in L6 rat skeletal myotubes [33]. Taken together, these results suggest that the alteration of the AMPK/Akt/mTOR pathway may play a role in the improvement of insulin resistance as well as damage of muscle fibers in the GMs of HFD-fed mice.

In conclusion, we showed that Ba decreased the plasma levels of glucose, insulin, and HOMA-IR, concomitant with macrophage infiltration and fibrotic areas in the GMs of HFD-fed SAMP8 mice. Furthermore, Ba treatment downregulated Akt and mTOR phosphorylation and upregulated AMPK phosphorylation in GMs. Although further investigation is required to clarify the detailed mechanism in aged SAMP8 mice, our study suggests that Ba may attenuate HFD-induced insulin resistance and chronic inflammation through modulation of the AMPK/Akt/mTOR pathway in the GMs of HFD-fed young SAMP8 mice. The treatment of Bangle could be a useful preventive strategy for obesity-related insulin resistance and may lead to improved hyperlipidemic and hyperglycolytic conditions in skeletal muscles.

Acknowledgements

The authors thank Keiko Tamakuma for providing technical assistance. This study was supported by a research grant (Shiteigata-grant) from Aomori University of Health and Welfare.

Statement of Competing Interests

The authors have no competing interests.

List of Abbreviations

AMPK, AMP-activated protein kinase; Ba, Bangle (*Zingiber purpureum*) extract; Con, SAMP8 control; GAPDH, glyceraldehyde-3-phosphate dehydrogenase; GM, gastrocnemius muscle; Glc, glucose; HFD, high-fat diet; HOMA-IR, homeostatic model assessment insulin resistance; IL-6, interleukin-6; LPS, lipopolysaccharide; mTOR, mammalian target of rapamycin; NEFA, non-esterified fatty acid; PI3K, phosphoinositide 3-kinase; Rcon, SAMR1 control; SAMP8, senescence-accelerated prone mice; Tg, triacylglycerol; TNF-α, tumor necrosis factor-α

References

[1] Oakes, N.D., Cooney, G.J., Camilleri, S., Chisholm, D.J. and Kraegen, E.W., "Mechanisms of liver and muscle insulin resistance induced by chronic high-fat feeding." *Diabetes*, 46 (11). 1768-1774, Nov 1997.

[2] Schenk, S., Saberi, M. and Olefsky, J.M., "Insulin sensitivity: modulation by nutrients and inflammation." *J Clin Invest*, 118 (9). 2992-3002, Sep 2008.

[3] Wu, H. and Ballantyne, C.M., "Skeletal muscle inflammation and insulin resistance in obesity." *J Clin Invest*, 127 (1). 43-54, Jan 3 2017.

[4] Patsouris, D., Cao, J.J., Vial, G., Bravard, A., Lefai, E., Durand, A., Durand, C., Chauvin, M.A., Laugerette, F., Debard, C., Michalski, M.C., Laville, M., Vidal, H. and Rieusset, J., "Insulin resistance is associated with MCP1-mediated macrophage accumulation in skeletal muscle in mice and humans." *PLoS One*, 9 (10). e110653, 2014.

[5] Andrianjafiniony, T., Dupre-Aucouturier, S., Letexier, D., Couchoux, H. and Desplanches, D., "Oxidative stress, apoptosis, and proteolysis in skeletal muscle repair after unloading." *Am J Physiol Cell Physiol*, 299 (2). C307-315, Aug 2010.

[6] Beyer, I., Mets, T. and Bautmans, I., "Chronic low-grade inflammation and age-related sarcopenia." *Curr Opin Clin Nutr Metab Care*, 15 (1). 12-22, Jan 2012.

[7] Huang, X., Liu, G., Guo, J. and Su, Z., "The PI3K/AKT pathway in obesity and type 2 diabetes." *Int J Biol Sci*, 14 (11). 1483-1496, 2018.

[8] Laplante, M. and Sabatini, D.M., "mTOR signaling in growth control and disease." *Cell*, 149 (2). 274-293, Apr 13 2012.

[9] Yoon, M.S., "The role of mammalian target of rapamycin (mTOR) in insulin signaling." *Nutrients*, 9 (11). 1176, Oct 27 2017.

[10] Khamzina, L., Veilleux, A., Bergeron, S. and Marette, A., "Increased activation of the mammalian target of rapamycin pathway in liver and skeletal muscle of obese rats: possible involvement in obesity-linked insulin resistance." *Endocrinology*, 146 (3). 1473-1481, Mar 2005.

[11] Saha, A.K., Xu, X.J., Lawson, E., Deoliveira, R., Brandon, A.E., Kraegen, E.W. and Ruderman, N.B., "Downregulation of AMPK accompanies leucine- and glucose-induced increases in protein synthesis and insulin resistance in rat skeletal muscle." *Diabetes*, 59 (10). 2426-2434, Oct 2010.

[12] Abdulmalek, S.A., Fessal, M. and El-Sayed, M., "Effective amelioration of hepatic inflammation and insulin response in high fat diet-fed rats via regulating AKT/mTOR signaling: Role of Lepidium sativum seed extracts." *J Ethnopharmacol*, 266. 113439, Feb 10 2021.

[13] Ruderman, N.B., Carling, D., Prentki, M. and Cacicedo, J.M., "AMPK, insulin resistance, and the metabolic syndrome." *J Clin Invest*, 123 (7). 2764-2772, Jul 2013.

[14] Liong, S. and Lappas, M., "Activation of AMPK improves inflammation and insulin resistance in adipose tissue and skeletal muscle from pregnant women." *J Physiol Biochem*, 71 (4). 703-717, Dec 2015.

[15] Zhao, L., Zou, T., Gomez, N.A., Wang, B., Zhu, M.J. and Du, M., "Raspberry alleviates obesity-induced inflammation and insulin resistance in skeletal muscle through activation of AMP-activated protein kinase (AMPK) alpha1." *Nutr Diabetes*, 8 (1). 39, Jul 2 2018.

[16] Nakai, M., Iizuka, M., Matsui, N., Hosogi, K., Imai, A., Abe, N., Shiraishi, H., Hirata, A., Yagi, Y., Jobu, K., Yokota, J., Kato, E., Hosoda, S., Yoshioka, S., Harada, K., Kubo, M., Fukuyama, Y. and Miyamura, M., "Bangle (*Zingiber purpureum*) improves spatial learning, reduces deficits in memory, and promotes neurogenesis in the dentate gyrus of senescence-accelerated mouse P8." *J Med Food*, 19 (5). 435-441, May 2016.

[17] Antunes, L.C., Elkfury, J.L., Jornada, M.N., Foletto, K.C. and Bertoluci, M.C., "Validation of HOMA-IR in a model of insulin-resistance induced by a high-fat diet in Wistar rats." *Arch Endocrinol Metab*, 60 (2). 138-142, Apr 2016.

[18] Sato, S., Kataoka, S., Sato, M., Takahashi, A., Norikura, T. and Mukai, Y., "Effect of Bangle (*Zingiber purpureum*) extract and low-intensity exercise on mTOR phosphorylation and autophagy flux in skeletal muscles of rats on a high-fat diet." *J Funct Foods*, 47. 554-561, Aug 2018.

[19] Winzell, M.S. and Ahren, B., "The high-fat diet-fed mouse: a model for studying mechanisms and treatment of impaired glucose tolerance and type 2 diabetes." *Diabetes*, 53 Suppl 3. S215-219, Dec 2004.

[20] Yamamoto, K., Kitano, Y., Shuang, E., Hatakeyama, Y., Sakamoto, Y., Honma, T. and Tsuduki, T., "Decreased lipid absorption due to reduced pancreatic lipase activity in aging male mice." *Biogerontology*, 15 (5). 463-473, 2014.

[21] Gungor, H., Ekici, M., Onder Karayigit, M., Turgut, N.H., Kara, H. and Arslanbas, E., "Zingerone ameliorates oxidative stress and inflammation in bleomycin-induced pulmonary fibrosis: modulation of the expression of TGF-beta1 and iNOS." *Naunyn Schmiedebergs Arch Pharmacol*, 393 (9). 1659-1670, Sep 2020.

[22] Abdi, T., Mahmoudabady, M., Marzouni, H.Z., Niazmand, S. and Khazaei, M., "Ginger (*Zingiber Officinale* Roscoe) extract protects the heart against inflammation and fibrosis in diabetic rats." *Can J Diabetes*, 45 (3). 220-227, Apr 2021.

[23] Kim, M.J. and Yun, J.M., "Molecular mechanism of the protective effect of zerumbone on lipopolysaccharide-induced inflammation of THP-1 cell-derived macrophages." *J Med Food*, 22 (1). 62-73, Jan 2019.

[24] Saltiel, A.R. and Olefsky, J.M., "Inflammatory mechanisms linking obesity and metabolic disease." *J Clin Invest*, 127 (1). 1-4, Jan 3 2017.

[25] Tzeng, T.F., Liou, S.S., Chang, C.J. and Liu, I.M., "The ethanol extract of Zingiber zerumbet attenuates streptozotocin-induced diabetic nephropathy in rats." *Evid Based Complement Alternat Med*, 2013. 340645, 2013.

[26] Tajik Kord, M., Pourrajab, F. and Hekmatimoghaddam, S., "Ginger extract increases GLUT-4 expression preferentially through AMPK than PI3K signalling pathways in C2C12 muscle cells." *Diabetes Metab Syndr Obes*, 13. 3231-3238, 2020.

[27] Deng, X., Zhang, S., Wu, J., Sun, X., Shen, Z., Dong, J. and Huang, J., "Promotion of mitochondrial biogenesis via activation of AMPK-PGC1a signaling pathway by Ginger (*Zingiber officinale* Roscoe) extract, and its major active component 6-gingerol." *J Food Sci*, 84 (8). 2101-2111, Aug 2019.

[28] Jing, Y., Wu, F., Li, D., Yang, L., Li, Q. and Li, R., "Metformin improves obesity-associated inflammation by altering macrophages polarization." *Mol Cell Endocrinol*, 461. 256-264, Feb 5 2018.

[29] Bodine, S.C., Stitt, T.N., Gonzalez, M., Kline, W.O., Stover, G.L., Bauerlein, R., Zlotchenko, E., Scrimgeour, A., Lawrence, J.C., Glass, D.J. and Yancopoulos, G.D., "Akt/mTOR pathway is a crucial regulator of skeletal muscle hypertrophy and can prevent muscle atrophy in vivo." *Nat Cell Biol*, 3 (11). 1014-1019, Nov 2001.

[30] Tang, H., Inoki, K., Brooks, S.V., Okazawa, H., Lee, M., Wang, J., Kim, M., Kennedy, C.L., Macpherson, P.C.D., Ji, X., Van Roekel, S., Fraga, D.A., Wang, K., Zhu, J., Wang, Y., Sharp, Z.D., Miller, R.A., Rando, T.A., Goldman, D., Guan, K.L. and Shrager, J.B., "mTORC1 underlies age-related muscle fiber damage and loss by inducing oxidative stress and catabolism." *Aging Cell*, 18 (3). e12943, Jun 2019.

[31] Wang, C.Y., Kim, H.H., Hiroi, Y., Sawada, N., Salomone, S., Benjamin, L.E., Walsh, K., Moskowitz, M.A. and Liao, J.K., "Obesity increases vascular senescence and susceptibility to ischemic injury through chronic activation of Akt and mTOR." *Sci Signal*, 2 (62). ra11, Mar 17 2009.

[32] Qian, S., Fang, H., Zheng, L. and Liu, M., "Zingerone suppresses cell proliferation via inducing cellular apoptosis and inhibition of the PI3K/AKT/mTOR signaling pathway in human prostate cancer PC-3 cells." *J Biochem Mol Toxicol*, 35 (1). e22611, Jan 2021.

[33] Den Hartogh, D.J., Vlavcheski, F., Giacca, A. and Tsiani, E., "Attenuation of free fatty acid (FFA)-induced skeletal muscle cell insulin resistance by resveratrol is linked to activation of AMPK and inhibition of mTOR and p70 S6K." *Int J Mol Sci*, 21 (14). 4900, Jul 11 2020.